ORIGINAL ARTICLE

Microfluidic focal thrombosis model for measuring murine platelet deposition and stability: PAR4 signaling enhances shear-resistance of platelet aggregates

K. B. NEEVES,*† S. F. MALONEY,*† K. P. FONG,‡§ A. A. SCHMAIER,‡¶ M. L. KAHN,‡¶ L. F. BRASS‡§ and S. L. DIAMOND*†

*Department of Chemical and Biomolecular Engineering; †Institute for Medicine and Engineering; ‡Department of Medicine; §Division of Hematology; and ¶Division of Cardiology, University of Pennsylvania, Philadelphia, PA, USA

Summary. *Background:* Flow chambers allow the *ex vivo* study of platelet response to defined surfaces at controlled wall shear stresses. However, most assays require 1–10 mL of blood and are poorly suited for murine whole blood experiments. *Objective:* To measure murine platelet deposition and stability in response to focal zones of prothrombotic stimuli using 100 μL of whole blood and controlled flow exposure. *Methods:* Microfluidic methods were used for patterning acid-soluble collagen in $100\ \mu m \times 100\ \mu m$ patches and creating flow channels with a volume of 150 nL. Within 1 min of collection into PPACK and fluorescent anti-mouse CD41 mAb, whole blood from normal mice or from mice deficient in the integrin α_2 subunit was perfused for 5 min over the patterned collagen. Platelet accumulation was measured at venous and arterial wall shear rates. After 5 min, thrombus stability was measured with a 'shear step-up' to 8000 s^{-1}. *Results:* Wild-type murine platelets adhered and aggregated on collagen in a biphasic shear-dependent manner with increased deposition from 100 to 400 s^{-1}, but decreased deposition at 1000 s^{-1}. Adhesion to patterned collagen was severely diminished for platelets lacking a functional $\alpha_2\beta_1$ integrin. Those integrin α_2-deficient platelets that did adhere were removed from the surface when challenged to shear step-up. PAR4 agonist (AYPGKF) treatment of the thrombus at 5 min enhanced aggregate stability during the shear step-up. *Conclusions:* PAR4 signaling enhances aggregate stability by mechanisms independent of other thrombin-dependent pathways such as fibrin formation.

Keywords: flow assay, microfluidics, murine platelets, thrombus stability.

Correspondence: Scott L. Diamond, Department of Chemical and Biomolecular Engineering and Institute for Medicine and Engineering, University of Pennsylvania, Philadelphia, PA, 19104, USA.
Tel.: +1 215 573 5704; fax: +1 215 573 6815.
E-mail: sld@seas.upenn.edu

Introduction

As anuclear cells, platelets are incompatible with *in vitro* genetic manipulation by transfection or transduction. Consequently, genetically modified mice are a critical tool for researchers studying the roles of platelet receptors and signaling in clot initiation, propagation and stability [1]. Chemical [2], photo-activated [3] and laser-induced [4] injury to vessels within genetically modified mice in combination with intravital microscopy [5] are powerful tools for capturing the complex interplay among platelets, endothelial cells and the subendothelial extracellular matrix. Yet, it is difficult to control or quantify the biochemistry of the wall injury within these models. In addition, local hemodynamic parameters such as wall shear stress are uncontrolled and can vary in vessel injury models.

Useful complements to *in vivo* models are *ex vivo* flow chambers that allow for manipulation of shear stresses [6–8], controlled presentation of platelet stimuli [9,10], and evaluation of pharmacological agents [11]. Flow chambers for studying platelet rolling, adhesion and aggregation over immobilized ligands have been critical in understanding shear-dependent receptor-ligand dynamics [12–14]. However, most parallel-plate and annular flow chambers require milliliters of fluid to perform experiments over a relevant time scale. This volume of blood is easily obtained from human subjects, but requires pooling or dilution of murine whole blood owing to the relatively low total blood volume of a single animal (∼1 mL) [15,16]. The cost of pooling and the sacrifice of difficult to breed animals can be prohibitive when using genetically modified mice to obtain data for a single experimental condition in a parallel plate flow chamber. Thus, current flow chamber designs are poorly suited for research with murine blood.

We developed a method for characterizing murine platelet function under flow using microfluidic and protein patterning techniques. This method addresses an important need for researchers who want to perform *ex vivo* flow assays using small volumes of blood from genetically modified mice. Owing

to the small size of the channels, the small volume (~100 μL) of blood obtained from a retro-orbital plexus was sufficient to perform an experiment, thus avoiding the need to sacrifice animals. We validated the method by measuring platelet adhesion to patterned collagen at venous and arterial wall shear rates and comparing platelet adhesion of wild-type mice and mice deficient in collagen receptors. The stability of platelet–collagen and platelet–platelet bonds was characterized by a high shear challenge. In addition, the role of PAR4 activation on aggregate stability was measured in a setting that was independent of fibrin formation.

Materials and methods

Fabrication of microfluidic devices

Microfluidic channels were fabricated in poly(dimethylsiloxane) (PDMS) using standard soft lithography techniques [17]. A detailed procedure of master fabrication and PDMS molding can be found in the Supporting Information. The devices for both protein patterning and blood flow used vacuum-assisted bonding to reversibly seal PDMS devices to glass slides [18] (Supporting Information). This reversible sealing method eliminated the need for plasma treating the PDMS to form a covalent bond and allows for *post hoc* analysis of platelet aggregates [19].

Microfluidic collagen patterning

Glass slides (75 × 50 × 1 mm, Fisherbrand, Fisher Scientific, Pittsburgh, PA, USA) were cleaned and functionalized with glutaraldehyde. A detailed procedure for functionalization of slides can be found in the Supporting Information. Functionalized slides were stored in HEPES buffered saline (HBS) at 4 °C until use. A PDMS mold with a single channel that ran along the length of the slide was vacuum bonded to treated slides. A solution of purified sterile bovine type I collagen (PureCol, 2.9 mg mL^{-1}, Inamed Biomaterials, Fremont, CA, USA) was introduced into the channel and allowed to form a thin film on the functionalized glass slide (Supporting Information). The collagen strip was stained with Texas Red so that the microscope could be focused prior to the introduction of blood. Texas Red staining was found to have no effect on platelet response (*not shown*). The collagen film was imaged by a multimode atomic force microscope (Digital Instruments, Inc., Santa Barbara, CA, USA) in tapping mode using a silicon cantilever (Veeco Probes, Camarillo, CA, USA) with a spring constant of 3 N m^{-1} and a tip radius of < 10 nm.

Mice

Flow assays were performed with whole blood from wild-type mice and mice deficient in one or both of the primary collagen receptors. Knockout mice deficient in the integrin α$_2$ subunit were generated as previously described [20]. A double knockout was created by crossing Fc receptor gamma chain (FcRγ)-

deficient mice (Taconic Farms, Hudson, NY, USA) with α$_2$-deficient mice [16]. Mixed background littermate animals were used as controls. All mouse studies were approved by the Institutional Animal Care and Use Committee (IACUC) of the University of Pennsylvania.

Blood collection and platelet labeling

Prior to blood draw, rat anti-mouse CD41 (GPIIb, α$_{IIb}$) monoclonal antibody (clone MWReg30, BD Biosciences, San Jose, CA, USA) was conjugated to Alexa Fluor® 488 using the Alexa Fluor® 488 Monoclonal Antibody Labeling Kit (Invitrogen, Carlsbad, CA, USA) according to the manufacturer's instructions. Whole mouse blood, obtained by intra-orbital eye bleed, was anti-coagulated with 93 μM (final concentration) Phe-Pro-Arg-chloromethylketone (PPACK, Haematologic Technologies Inc., Essex Junction, VT, USA) and labeled with 1:100 (v/v) Alexa-Fluor® 488-conjugated CD41 monoclonal antibody.

Whole blood flow assay

Channels were initially filled with 1 mg mL^{-1} BSA in HBS to ensure that no bubbles were trapped in the channel. Then, a volume of 100 μL of whole blood was placed on the inlet of the device and withdrawn by a syringe pump (Harvard Apparatus PHD 2000, Holliston, MA, USA) for 5 min at flow rates of 0.64, 2.5 and 6.4 μL min^{-1} to achieve full channel width-averaged wall shear rates of $\bar{\gamma}_{chan}$ = 100, 400, and 1000 s^{-1}, respectively. After 5 min of platelet accumulation on the collagen patch, the shear rate was stepped-up to an average wall shear rate of $\bar{\gamma}_{chan}$ = 8000 s^{-1} (50 μL min^{-1}) for 1 min to probe the stability of platelet aggregates.

Wall shear rate as a function of flow rate and position was calculated using an analytical solution of the velocity profile in a rectangular channel [21]:

$$u(y,z) = \frac{48Q}{\pi^3 hw} \times \frac{\sum_{n=1,3,5...}^{\infty} \frac{1}{n^3}\left[1 - \frac{\cosh\left(n\pi\frac{y}{h}\right)}{\cosh\left(n\pi\frac{w}{2h}\right)}\right]\sin\left(n\pi\frac{z}{h}\right)}{\left[1 - \sum_{n=1,3,5..}^{\infty}\frac{192h}{n^5\pi^5 w}\tanh\left(n\pi\frac{w}{2h}\right)\right]}$$

where $u(y,z)$ is the axial velocity at lateral location y and vertical position z in a channel of cross-sectional width w and height h ($^{-w}/2 \leq y \leq {}^{w}/2, 0 \leq z \leq h$) for a given volumetric flow rate Q.

Image capture and analysis

The adhesion, aggregation and fragmentation of platelets were monitored continuously by epifluorescence microscopy. Images were captured using a CCD camera (ORCA-ER Hamamatsu, Bridgewater, NJ, USA) mounted on an inverted microscope (Olympus IX81, Center Valley, PA, USA) with a 100 W mercury lamp (470 nm Ex/525 nm Em). Images were captured continuously at two frames per second (500 ms integration) using Slidebook software (Intelligent Imaging Innovations,

Denver, CO, USA). The use of a fluorescently labeled antibody allowed for continuous illumination of the field of view without additional adhesion, as has been reported using dye-loaded platelets [22]. The central 60 μm of the collagen patch (750 × 372 pixels) and a region upstream (50 × 372 pixels) of the collagen were defined using a custom MATLAB script (Mathworks Inc., Natick, MA, USA). The average background of the upstream region was calculated for each column and those values were subtracted from the reaction zone pixel values to correct for background gradients across the width of the channel. The background subtracted fluorescence intensity values were integrated over the collagen patch for each time point. Surface coverage was calculated by dividing the area of pixels with a value greater than zero by the area of the collagen patch.

Introduction of platelet agonists to formed platelet aggregates

For stability studies involving PAR activation, platelet aggregates were built up from PPACK-treated whole blood on patterned collagen for 5 min at 400 s⁻¹. After the deposition phase, the blood in the inlet was replaced with HBS. After 30 s of flow at the same average wall shear rate (400 s⁻¹), the buffer was then removed and replaced with 1 mM PAR4 agonist peptide (AYPGKF, Bachem, Torrance, CA, USA). Following 30 s of agonist presentation at 400 s⁻¹, the HBS flow rate was increased to provide an average wall shear rate of 8000 s⁻¹ to allow measurements of thrombus stability.

Statistical analysis

Each data point represented a single blood draw from one animal. All data are presented as mean ± SD. The Mann–Whitney U-test was used to compare wild-type blood perfused at 400 s⁻¹ (control) to each experimental group. Groups with P-values < 0.01 were considered significantly different from the control. All calculations were performed using the Statistics Toolbox in MATLAB.

Results

Platelet accumulation in microfluidic channels

In developing an *in vitro* analog of a focal vascular injury (albeit without thrombin), we perfused whole blood over a discrete region of immobilized collagen. A collagen thin film (width of ~15 nm were patterned within a microfluidic channel along the length of a glass slide (Fig. 1A,D). Thirteen individual channels with a cross-sectional area of 80 μm (height) × 100 μm (width) were oriented perpendicular to the collagen strip and vacuum-sealed to the slide (Fig. 1B,C). Table 1 summarizes the wall shear rates, genetic background, and sample size for each experimental condition.

Due to the low aspect ratio (the ratio of the cross-sectional width to the cross-sectional height, in this case 100/80μm, or 1.25) of the channels, the shear rate was non-constant along the channel walls. For example, at a flow rate of 2.5 μL min⁻¹ (whole channel width-averaged wall shear rate, $\bar{\gamma}_{chan} = 400$ s⁻¹), the shear rate had a parabolic profile on the bottom channel where it was zero in the corners and reached a maximum of 537 s⁻¹ in the middle (Fig. 2).

To eliminate wall effects, we only analyzed platelet accumulation within the middle 60 μm of the channel ($\bar{\gamma}_{central}$). Within this middle section of the channel, the range of the wall shear rate was small compared with the entire channel width (Table 1). This non-constant shear profile was reflected by the heterogeneous platelet distribution at average wall shear rates of 400 and 1000 s⁻¹ (Figs 3 and 4 and Supporting Movies SM1-3). Platelet accumulation was highest at low shear rates in the corners and less at positions in the middle of the channel at the highest shear rates, while the lowest shear rate did not exhibit the same preference towards the edges.
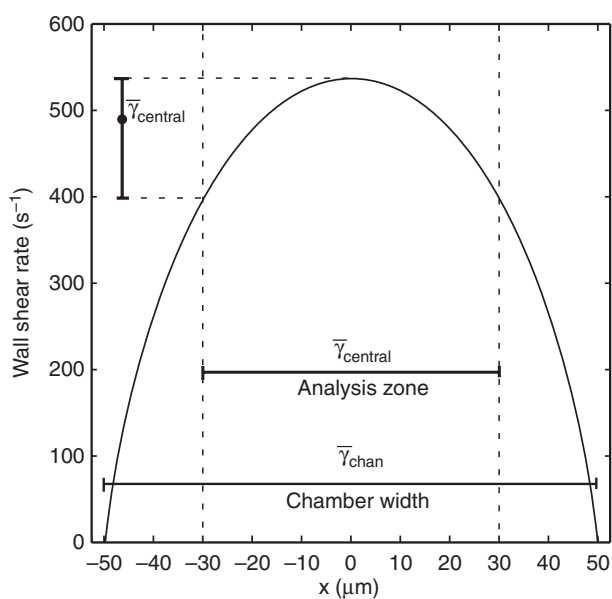
Platelet adhesion was not observed upstream or downstream from the collagen strip at any shear rate (Fig. 4). For wild-type mouse blood, there was a rapid rise in platelet accumulation for the first 3 min followed by minimal platelet deposition in the
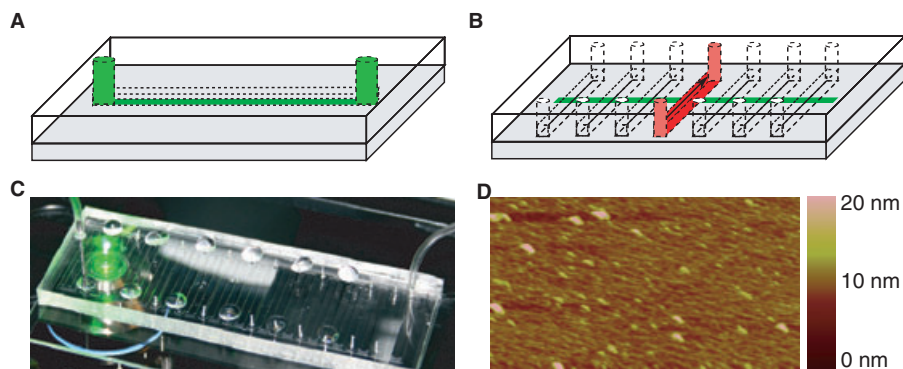
Fig. 1. Schematic of collagen patterning and blood flow experiments. (A) 100-μm strip of collagen was deposited and immobilized by microfluidic patterning along the length of a glass slide. (B) A second microfluidic device with a set of channels was oriented perpendicular to the patterned collagen. Murine whole blood was infused at an average wall shear rate of 100−1000 s⁻¹ for 4 min and the stability of platelet aggregates was tested by stepping-up the average wall shear to 8000 s⁻¹. (C) PDMS device with 13 microfluidic channels vacuum bonded to a glass slide. (D) Atomic force micrograph of patterned acid soluble type I collagen.

Table 1 Summary of experimental conditions for average wall shear for the entire channel ($\bar{\gamma}_{chan}$) and the central 60 μm of the channel ($\bar{\gamma}_{central}$), and the range of shear rates within the central 60 μm. Platelet accumulation, surface coverage and fragmentation calculations were based on the central 60 μm of the channel to exclude wall effects

Animal	$\bar{\gamma}_{chan}$ Average wall shear rate for entire channel (s^{-1})	$\bar{\gamma}_{central}$ Average wall shear rate in central 60 μm of channel (range) (s^{-1})	n
WT (C57BL/6)	100	126 (102–137)	7
WT (C57BL/6)	400	492 (399–537)	6
WT (C57BL/6)	1000	1260 (1021–1374)	6
WT (BalbC/ByJ)	400	492 (399–537)	8
$\alpha_2^{-/-}$	400	492 (399–537)	7
$\alpha_2^{-/-}/FcR\gamma^{-/-}$	400	492 (399–537)	6

Fig. 2. Wall shear rate distribution along the bottom of the microfluidic channel for an average wall shear rate of 400 s^{-1} ($\bar{\gamma}_{chan}$). The maximum shear rate is 537 s^{-1} in the middle of the channel. The dotted lines denote the central 60 μm of the channel that has a range of wall shear rates of 399–537 s^{-1} and an average wall shear rate of 492 s^{-1} ($\bar{\gamma}_{central}$). This central zone was used to calculate platelet accumulation and surface coverage.

fourth and fifth minutes (Fig. 5A). The dynamics of the platelet deposition curve was similar to those reported in the laser-induced vascular injury model [5]. We observed a delay of ~20 s followed by rapid platelet accumulation for 3–4 min. The time to saturation is about 50% quicker in the laser injury model, which is likely to be a result of thrombin generation, which was absent in these experiments due to the high concentration of PPACK.

Shear sensitivity of platelet deposition to patterned collagen

In the absence of preadsorbed vWF, we observed a biphasic response of platelet accumulation on patterned collagen (Supporting Movies SM1-3). After a 5-min perfusion over

collagen, there was significantly ($P < 0.01$) less platelet accumulation and surface coverage in the central zone ($\bar{\gamma}_{central}$) at 126 s^{-1} and 1260 s^{-1} compared with 492 s^{-1} (Fig. 5B). At an average wall shear rate of 126 s^{-1}, platelet adhesion was uniform across the width of the channel, but there were fewer platelet aggregates compared with 492 s^{-1}. At an average wall shear rate of 1260 s^{-1}, there was little platelet accumulation in the center of the channel. The few platelet aggregates that were observed may be due to adsorption of vWF from the plasma onto the collagen. While adsorption of vWF onto collagen from flowing mouse blood is expected during the experiment, platelet deposition will continually cover the collagen available for adsorption during the 300 s perfusion. The observed biphasic response illustrated in Fig. 5 was probably a result of competing effects where increasing flow increases the platelet flux to the collagen but also increases the force loading on adhesive bonds, reduces interaction times, and dilutes reactive species, resulting in less efficient platelet adhesion at higher flow rates.

For $\bar{\gamma}_{central} = 126$ s^{-1}, extending the perfusion time to 20 min did not result in increased platelet accumulation (Fig. S2). For these longer experiments, we observed continuous addition and removal of platelets, but there was no net change in the integrated fluorescent intensity after the first 300 s. These data suggest that the initial platelet layer on collagen dictated the final extent of thrombus growth in the absence of thrombin.

Accumulation of platelets with collagen receptor deficiencies

We performed flow experiments over patterned collagen with whole blood from mice deficient in one or both of the primary collagen receptors (Supporting Movies SM4 and SM5). Single knockout mice were deficient in the α_2 integrin subunit. A double knockout deficient in both FcRγ and α_2 was used as a negative control. The knockout mice have a mixed genetic background consisting of C57BL/6J, BalbC/ByJ and 129Sv/ImJ mice strains. Both C57BL/6J and BalbC/ByJ were used as wild-type controls. There was no statistical difference ($P = 0.75$) between platelet accumulation and aggregate fragmentation between the two wild-type controls (Fig. S1).

Platelets deficient in the α_2 integrin subunit had a diminished ability to adhere to patterned acid soluble collagen at an average wall shear rate of 400 s^{-1} (Fig. 6). There was a significant difference ($P = 0.0012$) in platelet accumulation for mice deficient in the α_2 integrin compared with wild-type mice. The small number of platelets that did adhere was presumably initiated through the GPIb-IX-V complex on platelets and vWF from the plasma adsorbed to the collagen. These data show that the $\alpha_2\beta_1$ receptor was necessary for firm adhesion to acid-soluble collagen under flow.

Thrombus stability and PAR signaling

A useful feature of flow chambers is the ability to control the shear rate and even change it within a single experiment.
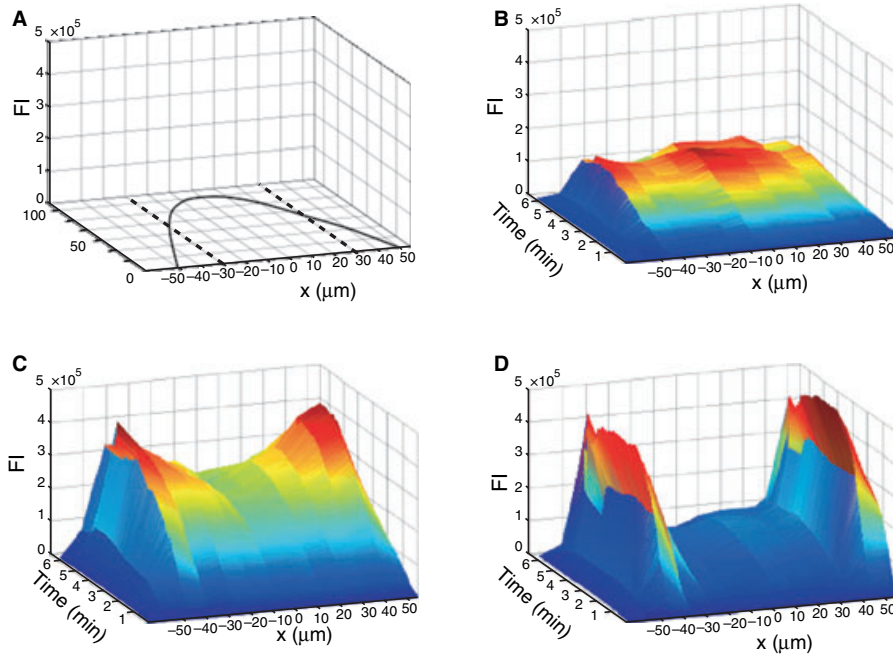
Fig. 3. The shear rate profile (A) dictated platelet accumulation as measured by fluorescence intensity (FI) in microfluidic channels for average wall shear rates of $\bar{\gamma}_{chan}$ = 100 (B), 400 (C), and 1000 (D) s^{-1}. The width of the channel was broken into 12 bins (10 × 100 μm) and the fluorescence intensity represents the average of each bin at each time point.
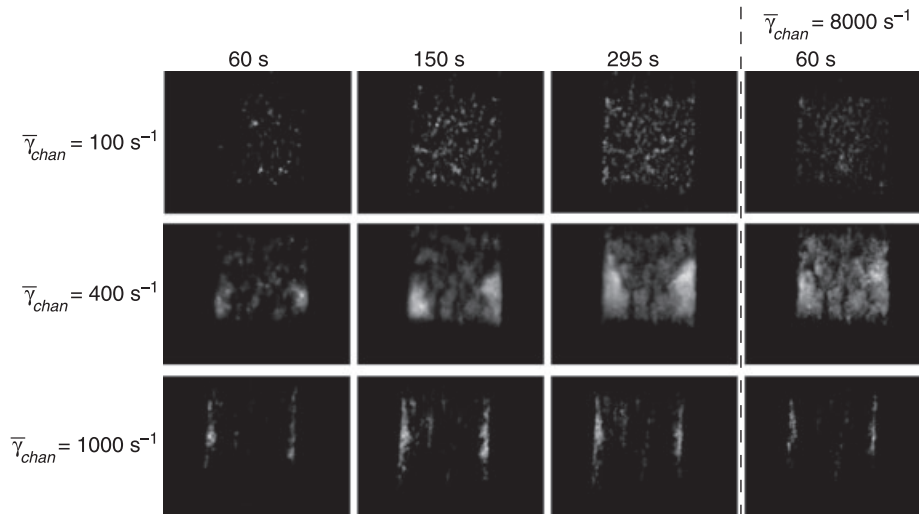
Fig. 4. Representative images of fluorescently labeled platelets accumulated on patterned immobilized type I collagen. These images were taken at the specified time points from experiments represented in the fluorescence traces shown in Fig. 5. Wild-type (C57BL/J6) platelets accumulated for 5 min at $\bar{\gamma}_{chan}$ = 100, 400 and 1000 s^{-1} and were subsequently challenged by a step-up to $\bar{\gamma}_{chan}$ = 8000 s^{-1} for 1 min. The direction of flow is from bottom to top.

Microfluidic chambers, due to their small volume, allow extremely high shear rates to be tested for extended periods of time even with very small volume whole blood samples. In each flow experiment, we monitored platelet accumulation for 5 min at a defined wall shear rate and then increased the average wall shear rate to $\bar{\gamma}_{chan}$ = 8000 s^{-1} for 1 min. Thrombus stability was defined by the percentage decrease in integrated fluorescence intensity and loss in surface coverage following the step-up in shear rate. During the 1-min exposure

of the preformed thrombus to ultra high shear rates of 8000 s^{-1} {a level known to cause shear-induced platelet activation (SIPA) in cone-and-plate viscometers [23]}, we found no indication that SIPA enhanced thrombus buildup during the 1-min exposure at 8000 s^{-1}. As seen in Figs 5(A) and 6, total fluorescence intensity drops by 15–25% for platelet deposits formed at venous and arterial shear rates. Platelets deficient in the α_2 subunit (single and double knockout) had a severe adhesion deficiency, covering less than 5% of the surface.
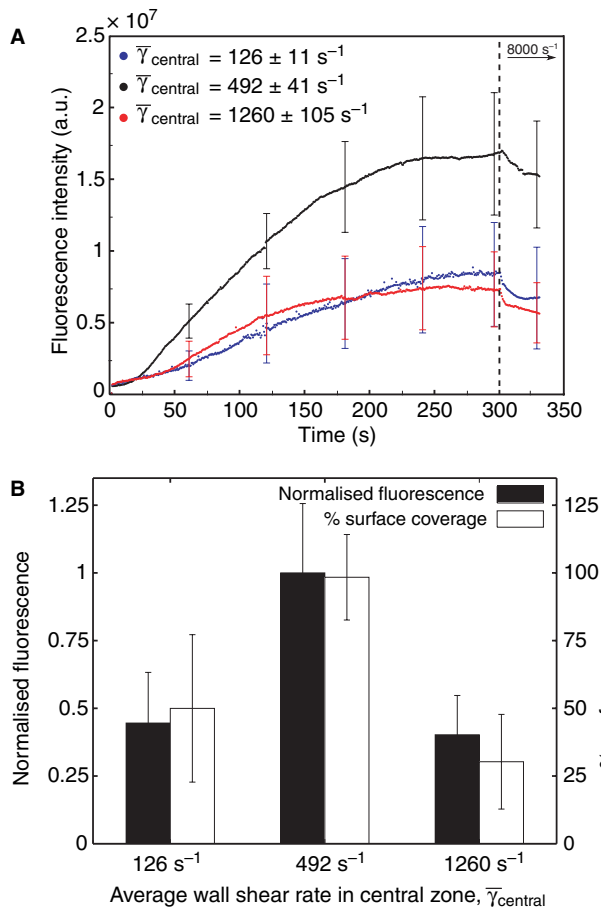
Fig. 5. Time traces of platelet accumulation on patterned collagen as a function of shear rate in the central 60 μm of the channel ($\bar{\gamma}_{central}$) (A). Error bars represent the standard deviation at $t = 60, 120, 180, 240, 295$ and 330 s for $n \geq 6$. Platelet accumulation for all experimental groups after perfusion over patterned collagen for 5 min (B). Platelet accumulation is expressed as integrated fluorescence intensity on the collagen patch relative to the accumulation at an average wall shear rate of 400 s^{-1}. Area coverage is expressed as percentage of interaction zone that had signal above background after 5 min of platelet accumulation.

Upon shear-up to 8000 s^{-1}, we observed essentially a complete removal of platelets from the surface (Fig. 6), demonstrating strict requirement for $\alpha_2\beta_1$ in stable firm adhesion to acid soluble type I collagen.

Thrombin is critical in clot formation and stability by distinct pathways involving platelet activation via protease activated receptor (PAR) signaling, enhanced recruitment of new platelets, and fibrin generation. In order to investigate mouse PAR4 signaling in the absence of active thrombin (which was blocked by 93 μM PPACK) and fibrin formation, we introduced an activating peptide after the platelet thrombus was formed to induce platelet signaling. By selectively infusing murine PAR4 activating peptide (AYPGKF) over preformed platelet aggregates, it was possible to determine the effect of PAR4 signaling on both platelet–collagen and platelet–platelet bond strength when subjected to a high shear challenge. PAR4 activation of platelets following accumulation on collagen led
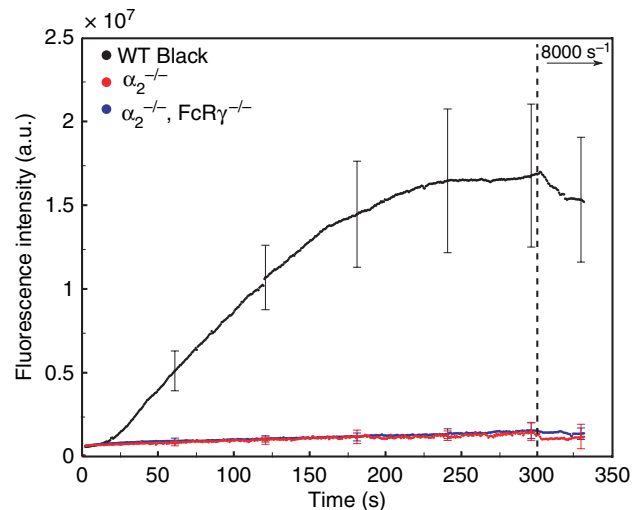
Fig. 6. Time traces of platelet accumulation on patterned collagen of wild-type and genetically modified mice in the middle 60 μm of the channel ($\bar{\gamma}_{central} = 492$ s^{-1}). Genetically modified mice were deficient in either one ($\alpha_2^{-/-}$) or both ($\alpha_2^{-/-}$, FcR$\gamma^{-/-}$) of the collagen receptors. Error bars represent the standard deviation at $t = 60, 120, 180, 240, 295$ and 330 s for $n \geq 6$.
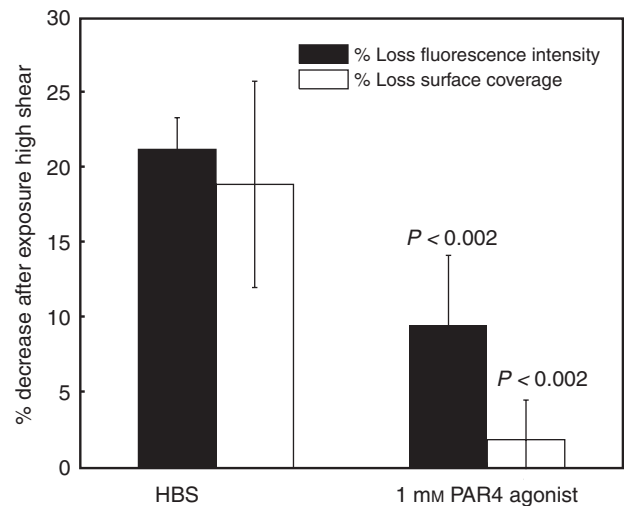
Fig. 7. Probing thrombus stability at high shear rates. The surface coverage and integrated fluorescence intensity on the collagen patch was measured immediately before and after exposure of an average wall shear rate of 8000 s^{-1} for 1 min. Percentage loss of total fluorescence intensity (FI) and area coverage following 1 min of high shear exposure (8000 s^{-1}) after platelet thrombus exposure to buffer control (HBS) or AYPGKF (PAR4 agonist) after accumulation at an average wall shear rate of 400 s^{-1}. Data are presented as the mean ($n \geq 6$) and the error bars represent the standard deviation.

to a stabilization of the thrombus compared with a buffer control (Fig. 7). There was a significant difference for both the percentage of total fluorescence intensity and area loss ($P = 0.002$) between the buffer control and the experimental group. While the initial size of each thrombus mass at 300 s may vary from mouse to mouse (as indicated in Fig. 5), we

found that every thrombi lost mass at 8000 s^{-1} and that the percentage decrease in mass was highly consistent. Because each and every thrombus formed, regardless of variations in its initial size at 300 s, displayed a decrease in fluorescence when exposed to 8000 s^{-1}, the percentage decrease in total fluorescence was measured to be 20 $\pm$ 3% ($n = 6$).

In Fig. 7, we report a 55% reduction in percentage loss with PAR4 agonist because an untreated thrombus has a $\sim$20% decrease in fluorescence intensity after exposure to 8000 s^{-1}, while a thrombus treated with PAR4 agonist has only a 10% decrease in fluorescence intensity. This decrease is statistically significant (21.3 $\pm$ 2.1% loss with buffer vs. 9.5 $\pm$ 4.7% loss with PAR4 agonist; $P < 0.002$, $n > 6$). In terms of % loss in surface coverage, we report in Fig. 7 a 90% reduction in percent surface loss with PAR4 agonist (18.9 $\pm$ 6.9% area loss vs. 1.9 $\pm$ 2.6% area loss with PAR4 agonist; $P < 0.002$, $n > 6$). Thus, regardless of the initial mass of the thrombus at 300 s (which can vary somewhat between mice as seen in the error bars of Fig. 6), each of these thrombi will lose about 20% of its volume when exposed to 8000 s^{-1} and this loss is substantially mitigated by 50% when the thrombi are exposed to a PAR4 agonist. While the total volume loss is only 20% with shear step-up to 8000 s^{-1} under these experimental conditions, the clinical significance of embolism is substantial and the results shown in Fig. 7 provide a quantitative *in vitro* method to interrogate thrombus stability. The increase in stability of mouse platelet aggregates was likely due to PAR4-mediated enhancement of both $\alpha_2\beta_1$-dependent platelet adhesion on collagen and $\alpha_{IIb}\beta_3$-dependent platelet–platelet interactions. Similar results were obtained in identical experiments performed with human platelet aggregates activated with the PAR1 agonist, SFLLRN (*not shown*), where 670 μM SFLLRN reduced percentage FI loss from 40% to 15% ($n = 8$, $P = 0.001$) compared with HBS control.

Discussion

Microfluidic techniques are ideally suited for *ex vivo* phenotyping of blood, especially when only small volumes are available, such as from genetically modified animals or in point-of-care diagnostic situations. The shear stress is a user-defined parameter in this microfluidic method that can be modulated during the course of an experiment. This feature allowed us to build up platelet aggregates at one shear rate and then probe the stability of platelet–ligand and platelet–platelet bonds at a higher shear rate. We detected disaggregation of wild-type mouse platelets during a shear-up challenge of 8000 s^{-1}. There was evidence of platelet–platelet and platelet–collagen bond failure, indicating instabilities at this pathological wall shear rate. Platelet deposition was shear dependent and biphasic (Fig. 5), revealing the competition of enhanced platelet delivery to the wall, reduced interaction times, and increased forces as flow increases. In α_2-deficient mice, those platelets that did adhere were almost completely removed after shear-up challenge, suggesting that stable adhesion to immobilized collagen was $\alpha_2\beta_1$ dependent. PAR4 activation led to increased stabilization to resist shear forces, suggesting a role for thrombin signaling in clot stability, independent of platelet recruitment or fibrin generation.

By manipulating the thrombin-driven platelet signaling independently of fibrin formation due to thrombin activity, it was possible to dissect the implications of PAR signaling on aggregate stability. PAR4 signaling significantly improved the ability of a focal collagen-initialized platelet thrombus to stay adhered in the face of a pathological shear force of 8000 s^{-1}. Measurements of loss of area coverage and total fluorescence intensity probed the stability of platelet–collagen ($\alpha_2\beta_1$) and platelet–platelet ($\alpha_{IIb}\beta_3$) following PAR4 signaling, respectively. We observed that PAR4 signaling increased the stability of the initially bound platelets to collagen (i.e. reduced the percentage surface coverage loss) as well as increased platelet–platelet stability.

In this report, we have scaled down the conventional flow chamber assay to a microfluidic platform. The salient advantage of this adaptation is the small volumes sufficient to run a flow experiment. Other reports of murine blood in *ex vivo* flow assays use either pool [15] or dilute [16,24] whole blood and often require the sacrifice of several animals. Dilution reduces plasma protein concentrations and alters the effect of red blood cells on platelet drift toward the wall. With a microfluidic system, no dilution or pooling was necessary to run a flow experiment over a relevant time frame for thrombosis via a non-lethal bleed. An important parameter for any *ex vivo* function test of platelets is the time between blood collection and the start of an experiment. A system requiring more than 100 μL of blood would entail a cardiac puncture and possibly the pooling of multiple animals. These procedures can take 10 min to 1 h depending on the number of animals and require the addition of other anticoagulants to ensure that platelets remain quiescent. In our system, the time from blood draw to platelet deposition in the image field was typically <1 min, an advantage in point-of-care diagnostic situations.

Microfluidic channels in combination with protein patterning more closely represent the focal nature of *in vivo* vascular injury than conventional flow chambers with uniformly coated surfaces. While parallel plate chambers are amenable to surface patterning proteins [25], they have higher volume requirements than microfluidic channels. In addition, blood flow in microfluidic channels more accurately mimics the hemodynamics found in arterioles and venoules [26,27]. Annular flow chambers such as capillaries have lower volume requirements, but are less amenable to discrete surface patterning with collagen. In configuration where proteins are adsorbed to the entire surface, there can be boundary layer depletion of platelets where adhesion decreases with axial position [28]. Due to the short length of the collagen patch in the direction of flow, platelet deposition was essentially uniform from the front of the patch to the back of the patch, especially within the central 60 μm region. Microfluidic techniques can be applied to explore several experimental conditions within a single device. For example, Gutierrez *et al.*[29] have developed a device to study platelet adhesion over a range of shear stresses (0.5–

50 dyne/cm^2), although without the focal patterning utilized in this system, with < 100 μL of whole blood.

Our patterning of acid soluble type I collagen yielded a homogeneous and repeatable thin film. Savage *et al.* [30] used blocking antibodies with human platelets and found that adhesion to acid soluble type I collagen under flow was dominated by $\alpha_2\beta_1$. Our observations that murine platelets deficient in the α_2 subunit cannot adhere to acid soluble collagen are consistent with these results. In contrast to soluble collagen, platelet arrest during flow over fibrillar collagen preferentially requires GPVI for adhesion and activation and demonstrates only a supporting role for $\alpha_2\beta_1$ [24]. While we used platelet–collagen interactions as a proof-of-principle in this report, micropatterning techniques can be extended to other prothrombotic molecules such as vWF [25,31], fibrillar collagen and tissue factor [32,33]. While fibrillar collagen is more physiological and has been tested in this system (*data not shown*), the active area in the device is so small that the number of collagen fibers per test area was highly variable. This is because deposition of fibrillar collagen was heterogeneous at the micron length scale. Consequently, we chose to use a homogeneous, reproducible collagen thin film for system characterization.

Conclusions

As thrombosis and hemostasis researchers continue to develop genetically modified animals and injury models, *ex vivo* assays need to adapt and evolve to complement features of the *in vivo* animal models. Flow-based assays are especially important because they mimic the shear stresses experienced by platelets in blood vessels. Here we applied microfluidic methods that have several advantages over conventional flow chambers, including: (i) low volume requirements (< 100 μL) that circumvent the need to dilute or pool murine whole blood, (ii) spatially defined presentation of a prothrombotic surface that mimics the focal nature of vascular injury with discrete boundaries at the injury site, and (iii) ability to probe thrombus stability at high shear stresses. These features allow a high number of replicates and may be useful for testing the pharmacological activity of small molecules or biologics in the presence of physiologically relevant flow.

Acknowledgements

Disclosure of Conflict of Interests

The authors state that they have no conflict of interest.

Supporting Information

Additional Supporting Information may be found in the online version of this article:

Figure S1. Genetic background does not alter platelet deposition response on collagen or stability during shear step-up. Platelet accumulation over patterned collagen for 300 s at an average wall shear rate of 400 s^{-1} for both black (C57B1/6) and white (BalbC/ByJ) wild-type mice, followed by a shear step-up test of stability at 8000 s^{-1}. Each data point is an average of six mice and error bars represent standard deviations.

Figure S2. Mouse platelet deposition at 100 s^{-1} on collagen reaches steady state within 400 s. Time traces of platelet accumulation on patterned collagen as a function of shear and time. For an $\bar{\gamma}_{chan} = 100$ s^{-1}, there was no net increase in platelet accumulation after 5 min. Data are presented as the mean ($n \geq 6$) and the error bars represent the standard deviation.

Figure S3. Schematic of photomask used for lithography. The white area outside the flow channels forms a vacuum groove in the final devices that is accessed by a vacuum tube (located at a position seen in the lower right corner of each mask). Black bars between the flow channels provide for stabilizing struts within the vacuum groove.

Figure S4. Photograph of finished silicon master wafer used for casting.

Figure S5. Schematic of the microfluidic protein patterning protocol used. Please refer to Supplemental section entitled 'Collagen patterning protocol' for details.

Video SM1. Representative video of wild-type black (C57BL/6) mouse platelets perfused at a volumetric flow rate of 0.64 μL min^{-1} ($\bar{\gamma}_{chan} = 100$ s^{-1}, $\bar{\gamma}_{central} = 126$ s^{-1}).

Video SM2. Representative video of wild-type black (C57BL/6) mouse platelets perfused at a volumetric flow rate of 2.5 μL min^{-1} ($\bar{\gamma}_{chan} = 400$ s^{-1}, $\bar{\gamma}_{central} = 492$ s^{-1}).

Video SM3. Representative video of wild-type black (C57BL/6) mouse platelets perfused at a volumetric flow rate of 6.4 μL min^{-1} ($\bar{\gamma}_{chan} = 1000$ s^{-1}, $\bar{\gamma}_{central} = 1260$ s^{-1}).

Video SM4. Representative video of $\alpha_2^{-/-}$ mouse platelets perfused at a volumetric flow rate of 2.5 μL min^{-1} ($\bar{\gamma}_{chan} = 400$ s^{-1}, $\bar{\gamma}_{central} = 492$ s^{-1}).

Video SM5. Representative video of $\alpha_2^{-/-}$ / FcR$\gamma^{-/-}$ mouse platelets perfused at a volumetric flow rate of 2.5 μL min^{-1} ($\bar{\gamma}_{chan} = 400$ s^{-1}, $\bar{\gamma}_{central} = 492$ s^{-1}).

Please note: Wiley-Blackwell are not responsible for the content or functionality of any supporting materials supplied by the authors. Any queries (other than missing material) should be directed to the corresponding author for the article.

References

1 Sachs UJ, Nieswandt B. In vivo thrombus formation in murine models. *Circ Res* 2007; **100**: 979–91.
2 Kurz KD, Main BW, Sandusky GE. Rat model of arterial thrombosis induced by ferric chloride. *Thromb Res* 1990; **60**: 269–80.

3 Matsuno H, Uematsu T, Nagashima S, Nakashima M. Photochemically induced thrombosis model in rat femoral artery and evaluation of effects of heparin and tissue-type plasminogen activator with use of this model. *J Pharmacol Methods* 1991; **25**: 303–17.

4 Rosen ED, Raymond S, Zollman A, Noria F, Sandoval-Cooper M, Shulman A, Merz JL, Castellino FJ. Laser-induced noninvasive vascular injury models in mice generate platelet- and coagulation-dependent thrombi. *Am J Pathol* 2001; **158**: 1613–22.

5 Falati S, Gross P, Merrill-Skoloff G, Furie BC, Furie B. Real-time in vivo imaging of platelets, tissue factor and fibrin during arterial thrombus formation in the mouse. *Nat Med* 2002; **8**: 1175–81.

6 Baumgartner HR. The role of blood flow in platelet adhesion, fibrin deposition, and formation of mural thrombi. *Microvasc Res* 1973; **5**: 167–79.

7 Sakariassen KS, Aarts PA, de Groot PG, Houdijk WP, Sixma JJ. A perfusion chamber developed to investigate platelet interaction in flowing blood with human vessel wall cells, their extracellular matrix, and purified components. *J Lab Clin Med* 1983; **102**: 522–35.

8 Sixma JJ, de Groot PG, van Zanten H, M IJ. A new perfusion chamber to detect platelet adhesion using a small volume of blood. *Thromb Res* 1998; **92**: S43–6.

9 Sakariassen KS, Joss R, Muggli R, Kuhn H, Tschopp TB, Sage H, Baumgartner HR. Collagen type III induced ex vivo thrombogenesis in humans. Role of platelets and leukocytes in deposition of fibrin. *Arteriosclerosis* 1990; **10**: 276–84.

10 Sakariassen KS, Muggli R, Baumgartner HR. Measurements of platelet interaction with components of the vessel wall in flowing blood. *Methods Enzymol* 1989; **169**: 37–70.

11 Kirchhofer D, Tschopp TB, Hadvary P, Baumgartner HR. Endothelial cells stimulated with tumor necrosis factor-alpha express varying amounts of tissue factor resulting in inhomogenous fibrin deposition in a native blood flow system. Effects of thrombin inhibitors. *J Clin Invest* 1994; **93**: 2073–83.

12 Ross JM, McIntire LV, Moake JL, Rand JH. Platelet adhesion and aggregation on human type VI collagen surfaces under physiological flow conditions. *Blood* 1995; **85**: 1826–35.

13 Balasubramanian V, Grabowski E, Bini A, Nemerson Y. Platelets, circulating tissue factor, and fibrin colocalize in ex vivo thrombi: real-time fluorescence images of thrombus formation and propagation under defined flow conditions. *Blood* 2002; **100**: 2787–92.

14 Goel MS, Diamond SL. Factor VIIa-mediated tenase function on activated platelets under flow. *J Thromb Haemost* 2004; **2**: 1402–10.

15 Konstantinides S, Ware J, Marchese P, Almus-Jacobs F, Loskutoff DJ, Ruggeri ZM. Distinct antithrombotic consequences of platelet glycoprotein Ibalpha and VI deficiency in a mouse model of arterial thrombosis. *J Thromb Haemost* 2006; **4**: 2014–21.

16 Sarratt KL, Chen H, Zutter MM, Santoro SA, Hammer DA, Kahn ML. GPVI and alpha2beta1 play independent critical roles during platelet adhesion and aggregate formation to collagen under flow. *Blood* 2005; **106**: 1268–77.

17 Duffy DC, McDonald JC, Schueller OJA, Whitesides GM. Rapid prototyping of microfluidic systems in poly(dimethylsiloxane). *Anal Chem* 1998; **70**: 4974–84.

18 Bang H, Lee WG, Park J, Yun H, Lee JSC, Cho K, Chung C, Han D, Chang JK. Active sealing for soft polymer microchips: method and practical applications. *J Micromech Microeng* 2006; **16**: 708–14.

19 Neeves KB, Diamond SL. A membrane-based microfluidic device for controlling the flux of platelet agonists into flowing blood. *Lab Chip* 2008; **8**: 701–9.

20 Chen J, Diacovo TG, Grenache DG, Santoro SA, Zutter MM. The alpha(2) integrin subunit-deficient mouse: a multifaceted phenotype including defects of branching morphogenesis and hemostasis. *Am J Pathol* 2002; **161**: 337–44.

21 White FM. *Viscous Fluid Flow*. New York, NY: McGraw-Hill Higher Education, 2006.

22 Haycox CL, Ratner BD, Horbett TA. Photoenhancement of platelet adhesion to biomaterial surfaces observed with epifluorescent video microscopy (EVM). *J Biomed Mater Res* 1991; **25**: 1317–20.

23 Shankaran H, Alexandridis P, Neelamegham S. Aspects of hydrodynamic shear regulating shear-induced platelet activation and self-association of von Willebrand factor in suspension. *Blood* 2003; **101**: 2637–45.

24 Nieswandt B, Brakebusch C, Bergmeier W, Schulte V, Bouvard D, Mokhtari-Nejad R, Lindhout T, Heemskerk JW, Zirngibl H, Fassler R. Glycoprotein VI but not alpha2beta1 integrin is essential for platelet interaction with collagen. *EMBO J* 2001; **20**: 2120–30.

25 Nalayanda DD, Kalukanimuttam M, Schmidtke DW. Micropatterned surfaces for controlling cell adhesion and rolling under flow. *Biomed Microdevices* 2007; **9**: 207–14.

26 Shevkoplyas SS, Gifford SC, Yoshida T, Bitensky MW. Prototype of an in vitro model of the microcirculation. *Microvasc Res* 2003; **65**: 132–6.

27 Higgins JM, Eddington DT, Bhatia SN, Mahadevan L. Sickle cell vasoocclusion and rescue in a microfluidic device. *Proc Natl Acad Sci U S A* 2007; **104**: 20496–500.

28 Sakariassen KS, Baumgartner HR. Axial dependence of platelet–collagen interactions in flowing blood. Upstream thrombus growth impairs downstream platelet adhesion. *Arteriosclerosis* 1989; **9**: 33–42.

29 Gutierrez E, Petrich BG, Shattil SJ, Ginsberg MH, Groisman A, Kasirer-Friede A. Microfluidic devices for studies of shear-dependent platelet adhesion. *Lab Chip* 2008; **8**: 1486–95.

30 Savage B, Ginsberg MH, Ruggeri ZM. Influence of fibrillar collagen structure on the mechanisms of platelet thrombus formation under flow. *Blood* 1999; **94**: 2704–15.

31 Okorie UM, Diamond SL. Matrix protein microarrays for spatially and compositionally controlled microspot thrombosis under laminar flow. *Biophys J* 2006; **91**: 3474–81.

32 Kastrup CJ, Runyon MK, Shen F, Ismagilov RF. Modular chemical mechanism predicts spatiotemporal dynamics of initiation in the complex network of hemostasis. *Proc Natl Acad Sci U S A* 2006; **103**: 15747–52.

33 Okorie UM, Denney WS, Chatterjee MS, Neeves KB, Diamond SL. Determination of surface tissue factor thresholds that trigger coagulation at venous and arterial shear rates: amplification of 100 fM circulating tissue factor requires flow. *Blood* 2008; **111**: 3507–13.